Corrosion behavior of pure magnesium processed by accumulative roll bonding for biomaterial application

Indah Suis Purnamasari[a*], Muhammad Rifai[b], Maman Kartaman Ajiriyanto[c], Ali Alhamidi[a], Mujamilah[b], Andon Insani[b], & Ahadi Damar Prasetya[b]

[a]Metallurgical Engineering, Faculty of Engineering, Universitas Sultan Ageng Tirtayasa, Banten 42435, Indonesia
[b]Center for Science and Technology of Advanced Material, National Nuclear Energy Agency, Banten 15314, Indonesia
[c]Center for Technology of Nuclear Fuel, National Nuclear Energy Agency, Banten 15314, Indonesia

Magnesium is one of the materials that can be used as an implant for the human body. It is because the daily intake of magnesium for an adult is 240-420 mg/day. Also, the elastic modulus (41 – 45 GPa) and density (1.74 g/cm^3) of magnesium is closer to that of natural bone. However, pure magnesium in the as-cast condition has a very fast corrosion rate, 2,89mmPY in 0.9% NaCl solution. Accumulative roll bonding (ARB) is done in this recent study to improve the corrosion rate of pure magnesium. ARB is one of the severe plastic deformations (SPD) method, which provides the possibility to obtain high strained materials without a macroscopic change after a cyclic roll-bonding process (stacking, preheating and rolling). Magnesium is annealed at 250°C and 350°C for 25 minutes, and then the ARB process is done with variation; one, two, three and four cycles. The composition was tested using SEM-EDS, showing that the content of a pure magnesium plate (as annealed) is 99.77%. The grain size is observed using the optic microscope and measured by ImageJ, while the corrosion rate was measured with an electrochemical and immersion test. The result showed the smallest grain size achieved is 7.204 ± 1,185 μm and that the lowest corrosion rate is 0,0012mmPY. The polarization resistance determined the thickness and the ability of passivation area obtained with the increasing number of ARB cycles. The higher plastic deformation is recommended for improve the corrosion resistance of the metallic material for future works.

Keywords: Magnesium, Accumulative roll bonding, Implant, Heat treatment, Corrosion rate

1 Introduction

The use of biomaterial has been studied for medical application such as orthopedic implant for the human body[1-5]. The orthopedic implant can be used for a fracture in the ankle, wrist, hip, and knee. Plates, screws, nails, pins, wires, and staples are types of implants that can be implanted in the bone to maintain mechanical integrity over 12-18 weeks while the bone tissue heals[6,7]. In the 1990s, gold and ivory were used for replacements of cranial defects. This was done by Egyptians and Romans that used polymethyl methacrylate (PMMA) for cranial defects[8,9]. Ever since, the use of metals as biomaterials accepted[6-9]. There are two types of biomedical implant for the human body[10-14], non-degradable implant and biodegradable implant. The non-biodegradable implant is a permanent implant inside the body with a risk of inflammation[10,11]. It also needs another operation to eliminate the implant from the body. At the same time, the biodegradable implant can degrade naturally inside the body after the tissue has healed, so it does not need a follow-up operation to eliminate the implant from the body[12-14].

In 1878, the first clinical application was made by physician Edward C. Huse, where magnesium wire ligatures were used to stop bleeding vessels successfully[10,14]. However, a further study found that magnesium had a high corrosion rate, about 2,89mmPY in 0.9% NaCl also had a limited mechanical property[10]. Magnesium degraded too quickly, and hydrogen gas in implant becomes the main concern for magnesium as an implant, compared to titanium and stainless steel[15-18].

Severe Plastic Deformation (SPD) is defined as a metal forming process that used an ultra-large plastic strain to create an ultrafine-grained metal[19-23]. Accumulative roll bonding (ARB) is one of SPD's processes that can produce ultrafine-grained metals by doing continuous rolling without changing the geometrical changes to the metals[24-27]. ARB was done by dividing the sheet into two pieces (of the same size) then cleaned the surface. After that, the sheets were stacked and rolled. The rolling can be done

with more than a cycle to achieve an ultra-high plastic strain so that it can enhance the mechanical properties and corrosion resistance of the materials. Pure magnesium sheet can be rolled with the ARB process to achieve an ultra-fine grained[28-32]. The previous researcher stated that a grain size refinement could be done for magnesium to achieve a corrosion rate of less than 0.5 mmPY in simulated body fluid (SBF)[33-37]. The purpose of this study is to investigate the effect of ARB process on corrosion behavior.

2 Materials and Methods

The material used for the ARB process was pure magnesium ingot (99.77% Mg) which cut into a sheet with the size of 150 × 34 × 2.2 mm. The schematic illustration of the ARB process is shown in Fig. 1. The sheet was annealed under its recrystallization temperature, 400°C, for an hour. The specimens were as annealed pure magnesium sheet. The specimen was divided into two become 75 x 34 x 2.2 in size. The code system for specimens shown in Table 1.
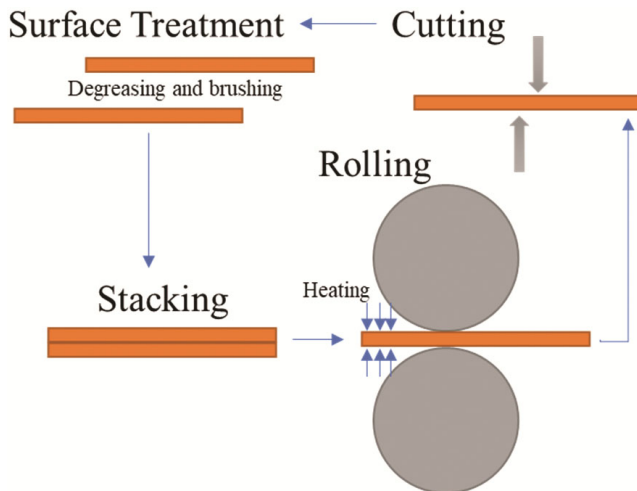

Fig. 1 — Schematic process of ARB.

Table 1 — Code System for Specimens

Sample Code	Temperature (°C)	Cycle	Reduction (%)
Mg 0	400		*as annealed*
250-S1S		1	
250-S2S	250	2	
250-S3S		3	
250-S4S		4	50
350-S1S		1	
350-S2S	350	2	
350-S3S		3	
350-S4S		4	

The surface of the pure mg sheet was ground with 1000 grit abrasive paper then cleaned with acetone to remove the dirt. The two sheets were stacked with the help of copper wire on every corner of the sheet. Then the specimen was annealed in a furnace for 25 minutes with the variation of temperature; 250°C and 350°C. The ARB experiments were conducted with a ±10 ton of "roll load" at a rolling speed of 26 rpm without lubrication. Percentage reduction of the specimens was 50 %, with the variation of cycles observed were 1, 2, 3 and 4 cycles.

The microstructure of ARB processed pure magnesium sheets was observed by optical microscope and scanning electron microscopy (SEM). And for the corrosion behavior of ARB processed, pure magnesium sheets were investigated by two methods: immersion test, electrochemical test. The test was conducted in simulated body fluid (SBF) solution. Two kinds of electrochemical test, namely the potentiodynamic polarization test and electrochemical impedance spectroscopy (EIS) test, were carried out to compare corrosion resistance of pure magnesium sheet specimens.

3 Results and Discussion

The microstructural examination was conducted as annealed and as ARB processed pure magnesium specimens by optical microscopy and the grain size calculated by an ImageJ. The mean grain size of pure magnesium specimens shown in Table 2. From the data, it can be known that the grain size after one cycle of ARB significantly reduced to 21,591 ± 13,118 µm with the help of the plastic deformation, which made the bigger size of grain shattered into the smaller one.

Figures (2 and 3) shows optical microstructures of pure magnesium specimen before ARB (Figs. 2(a) and 3(a)) and ARB-processed for various cycles (Figs. 2(b) - (i) and 3(b) - (c)). The as-annealed

Table 2 — Grain Size of Pure Magnesium Plate

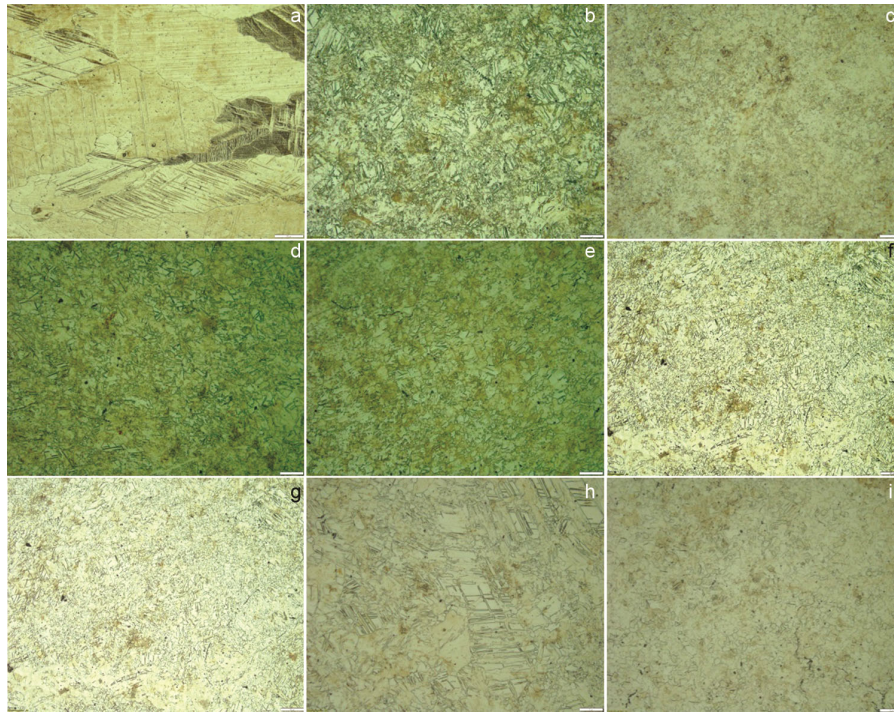| Sample Code	Mean Grain Size (µm)
Mg 0	145,381 ± 16,843
250-S1S	21,591 ± 13,118
250-S2S	13,575 ± 6,149
250-S3S	7,204 ± 1,185
250-S4S	7,947 ± 1,948
350-S1S	31,759 ± 16,152
350-S2S	18,737 ± 8,859
350-S3S	9,753 ± 2,752
350-S4S	9,753 ± 2,752

Fig. 2 — Optical microstructure of pure magnesium sheet before and after ARB process (a) as annealed, (b) 250-S1S, (c) 250-S2S, (d) 250-S3S, (e) 250-S4S, (f) 350-S1S, (g) 350-S2S, (h) 350-S3S, and (i) 350-S4S.
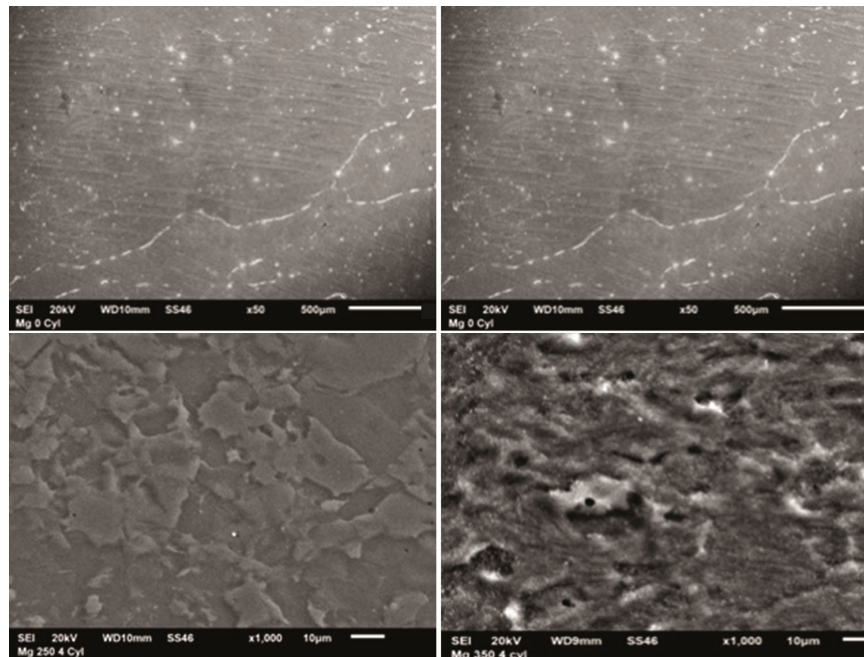

Fig. 3 — SEM images before and after ARB process (a) as annealed (500X), (b) 250-S4S (1000X), and (c) 350-S4S (1000X).

samples contained equiaxed grain. As can be seen from Fig. 2(b), fine elongated grains are developed after one cycle of ARB. However, the microstructure is far from homogeneous, but as the number of ARB cycles increases, the microstructure becomes finer.

Figure 4 shows a relationship between grain size and the increasing number of ARB cycles pure magnesium specimens. As seen in Table 2 and Fig. 4, the specimens in 250°C have a smaller grain size compared to specimens in 350°C. It is because if

ARB were performed at elevated temperatures, at which enough slip systems become active, rapid grain growth takes places, making it difficult to obtain ultrafine-grained microstructure in magnesium.

Fig. 5 represents relationship between immersion times with corrosion rate of pure magnesium specimens.

Fig. 6 represents relationship between ARB cycles and corrosion Rate measured by electrochemical test.

For samples in 250°C temperature, the smallest grain size is achieved in the third cycles around 7,204 ± 1,185 μm meanwhile the biggest grain size is achieved by the first cycle around 21,591 ± 13,118
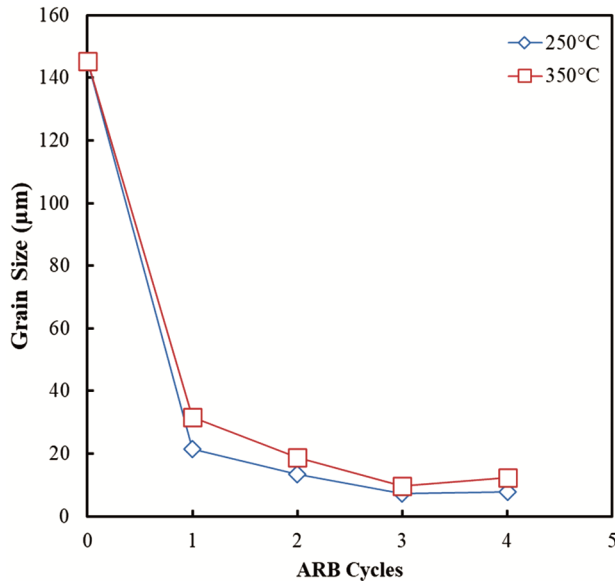

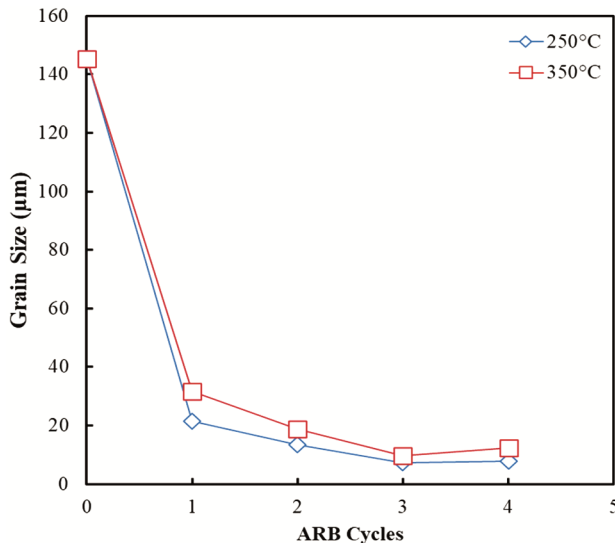Fig. 4 — Relationship between ARB cycles and grain size of pure magnesium specimens.

Fig. 5 — Relationship between immersion times with corrosion rate of pure magnesium specimens.

μm. And for samples in 350°C temperature, the smallest grain is achieved in the third cycles around 9,753 ± 2,752 μm while the biggest grain size is achieved by the first cycle around 31,759 ± 16,152 μm.

As shown in Fig. 4, after the first pass, the grain size significantly reduced because of the shear strain induced by the ARB process. Hence, more ARB passes led to a slight decrease in grain size. Besides, the increase of grain size on the fourth cycles is because critical minimum grain size is achieved. Thus, the subsequent cycles do not have any important refining effects. This is attributed to the incomplete dynamic recrystallization followed by grain growth due to the residual accumulated strain energy.

The corrosion rate of pure magnesium specimens can be calculated through an immersion test followed by a weight-loss method. Pure magnesium specimens were immersed in simulated body fluid (SBF) solution at 37°C temperature for 24 hours. Table 3 shows a corrosion rate of pure magnesium specimens calculated using Equation 1[10]:

$$C.R. = \frac{534 \times w}{A \times T \times D} \qquad \qquad ...(1)$$
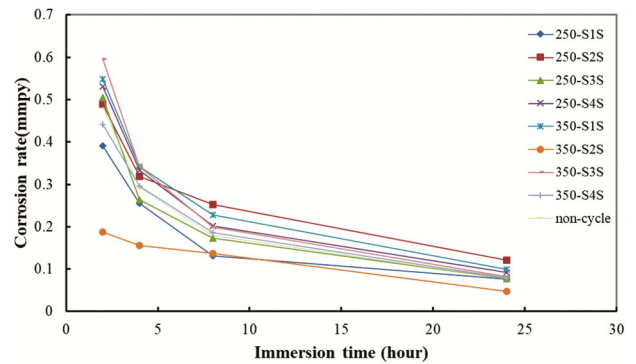

Fig. 6 — Relationship between ARB cycles and corrosion Rate measured by electrochemical test.

Tabel 3 — Corrosion Rate of Samples				
Sample	Corrosion Rate (mmpy)			
	2 hours	4 hours	8 hours	24 hours
Mg 0	0,480293	0,292319	0,180302	0,077491
250-S1S	0,009939	0,006470	0,003332	0,001926
250-S2S	0,012433	0,008087	0,006412	0,003082
250-S3S	0,012823	0,006704	0,004414	0,001994
250-S4S	0,013486	0,008458	0,005125	0,002358
350-S1S	0,01391	0,00869	0,00579	0,00253
350-S2S	0,00476	0,00398	0,00348	0,0012
350-S3S	0,01512	0,00869	0,00472	0,03414
350-S4S	0,01123	0,0075	0,00472	0,00203

Table 4 — Result of Rp and Ru by EIS		
Sample	Rp (ohm)	Ru (ohm)
250-S1S	3835	84,10
250-S2S	2560	91,25
250-S3S	3557	80,14
250-S4S	4373	73,60
350-S1S	6049	78,15
350-S2S	2334	90,06
350-S3S	3700	98,86
350-S4S	1572	90,39

where, *CR* is corrosion rate (mpy), *A is* surface area (cm^2), *T is* time (hours) and *D*is density (g/cm^3).

From Table 4, a graph that shows the relationship between immersion time and corrosion rate can be illustrated in Fig. 5. It shows that the corrosion rate reduced with the increasing immersed time of specimens in SBF solution. Table 2 shows the lowest corrosion rate from specimens in 250°C is 250-S2S. The specimens were heated to 350°C temperature. This phenomenon can be affected by the degradation behavior, which is influenced by impurities in specimens and the physiological environments such as the concentration of HCO^{3-} in SBF solution alters the corrosion rate of pure magnesium. The previous study showed the reaction between Ca^{2+} and HCO^{3-} in SBF solution influenced the reaction between Mg^{2+} and HCO^{3-} because it slowed down the formation of protective film on top of MgO/Mg(OH)$_2$ layer[10].

Aside from the immersion test, an electrochemical test can be used to measure the corrosion rate of pure magnesium specimens. An electrochemical test was performed to get accurate electrochemical data of ARB processed pure magnesium. The relationship of ARB cycles and corrosion rate measured by the electrochemical test.

As seen in Fig. 6 that the corrosion rate keeps increasing until the third cycles for both 250°C and 350°C specimens. For specimens processed in 250°C temperature, the lowest corrosion rate is achieved by 250-S4S for 0,05908 mmPY, while for specimens processed in 350°C temperature is achieved by 350-S1S for 0,069444 mmPY. For the highest corrosion rate is achieved by 250-S3S for specimen processed in 250°C temperature and 350-S3S for specimens processed in 350°C temperature.

The previous study use ARB process under 250°C and 350°C temperature for a pure magnesium sheet showed that the lowest residual stress achieved by specimens processed under 350°C temperature, which predicted that the corrosion rate for it would lower
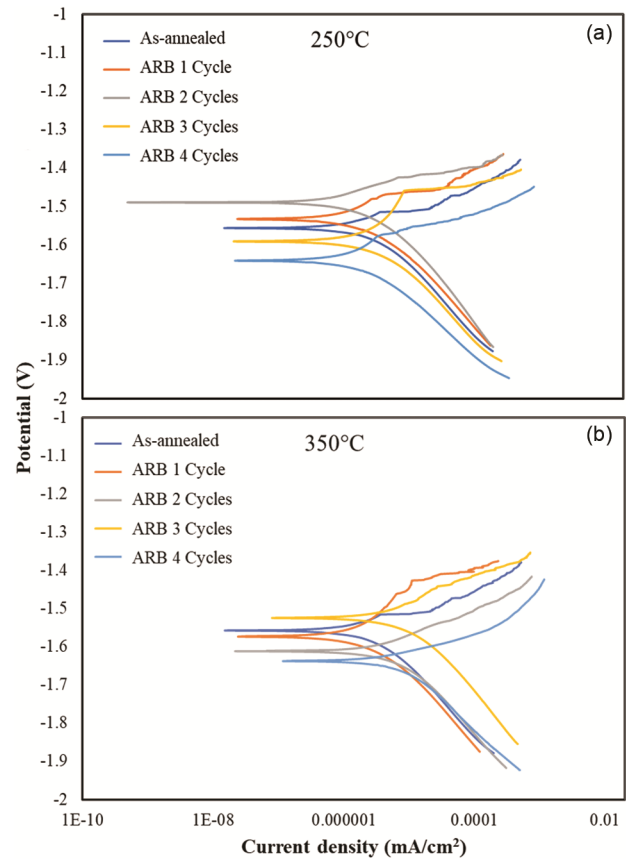

Fig. 7 — Polarization curve of (a) 250°C, and (b) 350°C temperature process.

than specimens processed under 250°C temperature[26]. This statement supported by previous researcher that stated the corrosion rate would decrease with a decrease of residual stresses on the material[34]. Compared to the data from the previous researcher, this recent study showed that the specimens processed under 350°C has a higher corrosion rate than 250°C temperature. The previous researcher proposed the influence of residual stress on corrosion resistance is relatively less evident and outweighed by grain size[34]. The residual stresses could increase the anodic polarization current densities[38-42].

Figure 7 shows an accelerated anodic process could lead to reduced corrosion resistance. In theory, microscale residual stress can reduce the activation energy for an atom to leave the metal lattice and get into the solution. Based on the mean grain size that achieved, the third cycles specimen, 350-S3S, has the highest corrosion rate while it has the smallest mean grain size. This could happen because there was different friction between specimen and roll. Also, the velocity of rolling was not optimum, which caused the grain refinement did not happen homogenously.

The microstructural examination was conducted to observe a corrosion product on Mg 0, 350-S1S and 350-S3S specimens. There is corrosion on the specimen's surface which shown by holes that existed. Also, the area was darker. In Fig. 8, the corrosion area was highlighted with a red circle. As shown, the corrosion product on the 350-S1S specimen's surface was produced more than Mg 0 specimen. Meanwhile, for the 350-S3S specimen, there were cavities on its surface, which is worse than those produced in Mg 0 and 350-S1S specimens. From this, it is known that 350-S3S produced the most corrosion product on its surface, which made it had a high corrosion rate, as shown in Fig. 8.

An electrochemical impedance spectroscopy (EIS) test was done to know corrosion resistance through an impedance curve. Impedance curve, polarization resistance and solution resistance were the data that obtain from the EIS test. The polarization resistance determined the thickness and the ability of passivation area obtained with the increasing number of ARB cycles, which means the resulted strain will increase with the increasing number of ARB cycles[43-45]. Theoretically, the increasing number of ARB cycles will increase the

value of equivalent strain and Rp value but decrease the corrosion rate.

Figure 9 is a graph of *Rp* and equivalent strain in every cycle of the ARB process. The present data was compared to ECAP, and HPT processed sample[46,47]. As shown in Fig. 9, the influence of equivalent strain to *Rp*. For ARB processed in 250°C and HPT, ZK60 had a similarity, which is the decrease of earlier cycles, but after the third cycles, the Rp value was increasing. Meanwhile, for ARB processed at 350°C and ECAP pure magnesium keep decreasing with the increasing number of cycles. The previous researcher stated the decreasing of Rp value with the increasing number of ECAP is because crystalline defects formed during the ECAP process accelerated the formation of passivation film, which triggered a corrosion reaction to take place. That is why the corrosion rate of ECAP pure magnesium specimens was lower than the as-cast one.

Figures (10 and 11) are a Nyquist curve or an impedance curve of pure magnesium sheet before and after the ARB process. The impedance curve showed

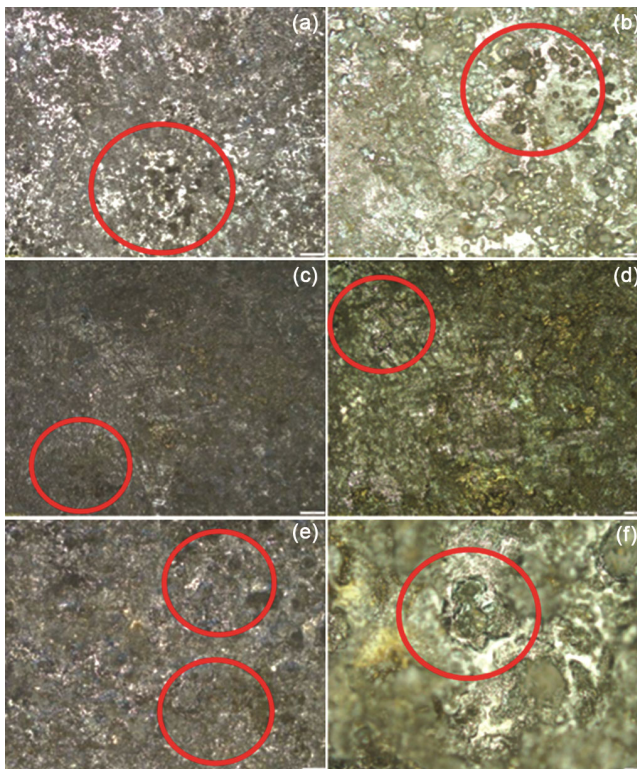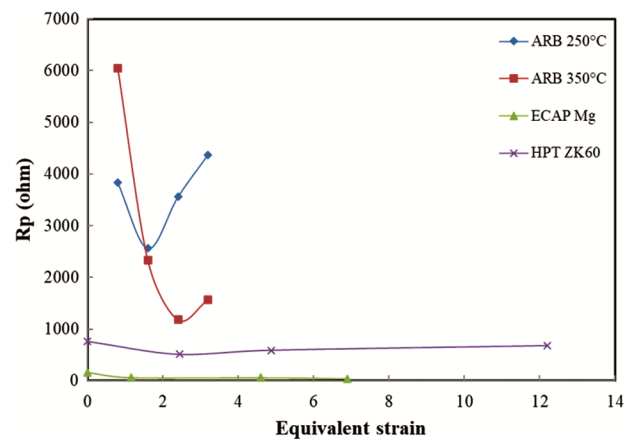Fig. 9 — Relationship between Rp and equivalent strain.

Fig. 8 — Optical microstructure of corrosion product (a) Mg 0 (50X), (b) Mg 0 (100X), (c) 350-S1S (50X), (d) 350-S1S (100X), (e) 350-S3S (50X), and (f) 350-S3S (200X).
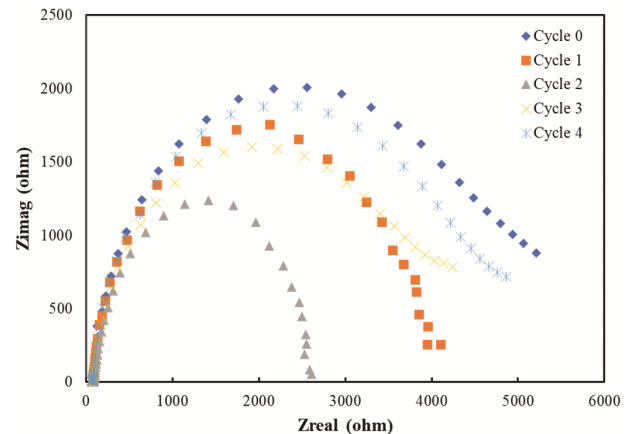
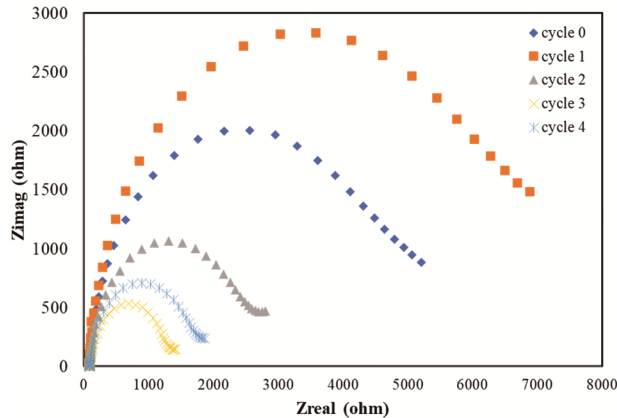Fig. 10 — Impedance curve of 250 °C specimens.

Fig. 11 — Impedance curve of 350 °C specimens.

one capacitive loop that happened in a high frequency; it showed that Mg^{2+} dissolve in the solution then formed an oxide film on the surface. The previous researcher stated that the bigger the diameter loop on the curve, the higher number of ARB cycles and the lower of corrosion rate achieved.

Figure 10 show that the 250-S4S specimen has the highest *Rp* value and the biggest diameter loop. This indicated that the 240-S4S specimen had the lowest corrosion rate compared to all specimens processed under 250°C temperature. While for specimens under 350°C ARB process, the highest *Rp* value and the biggest diameter loop achieved by the 350-S1S specimen, which indicated that 350-S1S specimen had the lowest corrosion rate among 350°C specimens.

Based on Fig. 11, it shows that specimen processed under 250°C temperature had a decrease *Rp* value and diameter loop until the second cycles, and after that, it keeps increasing. While for 350°C specimens, the decreasing of Rp value and diameter loop happened until the third cycles and increased on the fourth cycles. The decreasing of corrosion rate after it keeps increasing is caused by an ultrafine-grained structure that had just formed on those cycles. Severe plastic deformation could control the microstructure evolution and corrosion behavior, so the application for orthopedic could be controlled properly. The corrosion behavior of magnesium could be studied in detail using several solutions that could simulate the usage of magnesium in the body, such SBF and DMEM. Another severe plastic deformation techniques like high pressure torsion and equal channel angular pressing could be done to improve the ARB results.

4 Conclusion

Based on the result and discussion above, we can conclude that: The smallest grain size achieved by 250-S3S for 7,204 ± 1,185 μm. The lowest corrosion rate achieved by 350-S2S for 0,0012mmPY. An optimum annealing temperature in the ARB process is at 350°C because it achieved the lowest corrosion rate in the second cycles.The polarization resistance determined the thickness and the ability of passivation area obtained with the increasing number of ARB cycles. The higher plastic deformation, such high-pressure torsion and equal channel angular pressing are recommended for improve the corrosion resistance of the metallic material for future works.

References

1 Agarwal Rachit, & Andrés JGarcía, *Adv Drug Deliv Rev,* 94 (2015) 53.
2 Asselli A A C, Leiva D R, Huot J, Kawasaki M, Langdon T G, &Botta W J, *Int J Hydrog Energy,* 40.47 (2015) 16971.
3 Atrens, Andrej, Song Guang-Ling, Liu Ming, Shi Zhiming, Cao Fuyong, &Dargusch Matthew S, *Adv Eng Mater,* 17.4 (2015) 400.
4 Bahmani, Ahmad, Srinivasan Arthanari, & KwangSeon Shin, *J Magnes Alloy,* 8.1 (2020) 134.
5 Cao Yang, Ni Song, Liao Xiaozhou, Song Min, & Zhu Yuntian, *Mater Sci Eng R Rep,* 133 (2018) 1.
6 Banerjee Parama Chakraborty, Al-SaadiSaad, Choudhary Lokesh, Harandi Shervin Eslami, & Singh Rama, *Materials,* 12.1 (2019) 136.
7 Cheepu Muralimohan, Haribabu S, Ramachandraiah T, Srinivas B, Venkateswarulu D, Karna Sivaji, AlapatiSuresh, & CheWoo Seong, *Appl Mech Mater*, 877(1) (2018) 183.
8 ChenYongjun, Xu Zhigang, Smith Christopher, & Sankar Jag, *Acta Biomater,* 10.11 (2014) 4561.
9 Curioni M, Sceninia F, Monettab T, & Bellucci F, *Electrochim Acta,* 166 (2015) 372.
10 Demir Ali Gökhan, Lorenzo Monguzzi, & Barbara Previtali, *Addit Manuf,* 15 (2017) 20.
11 Esmaily M, Svensson J E, Fajardo S, Birbilis N, Frankel G S, Virtanen S, Arrabal R, Thomas S, & Johansson L G, *Prog Mater Sci,* 89 (2017) 92.
12 Estrin Yuri, & Alexei Vinogradov, *Acta Mater,* 61.3 (2013) 782.
13 FathyAdel, Ibrahim Dalia, Elkady Omayma, & Hassan Mohammed, *J Compos Mater,* 53(2) (2019) 209.
14 Ge Mao-Zhong, Xiang Jian-Yun, Yang L, & Wang J T, *Surf Coat Technol,* 310 (2017) 157.
15 GrünNicole G, Holweg P, Tangl S, Eichler J, Berger L, Beucken J JJ P van den, Löffler J F, Klestil T, & Weinberg A M, *Acta Biomater,* 78 (2018) 378.
16 HallabNadim James, &Jacobs Joshua J, *BiomaterSci*, (2020) 1079.
17 Hosaka Taito, Yoshihara Shoichiro, AmaninaIman, & Macdonald Bryan J, *Procedia Eng,* 184 (2017) 432.
18 Inzana Jason A, Schwarz Edward M, Kates Stephen L, & Awad Hani A, *Biomaterials,* 81 (2016) 58.

19 Jafari Sajjad, Harandi Shervin Eslami, & Raman RK Singh, *Jom,* 67(5) (2015) 1143.

20 Kamrani Sepideh, & Fleck Claudia, *Biometals,* 32(2) (2019) 185.

21 Li Long, Zhang Ming, Li Ye, Zhao Jie, Qin Ling, & Lai Yuxiao, *Regen Biomater,* 4(2) (2017) 129.

22 Li X C, Zhang Y K, Chen J F, & Lu Y L, *Mater Sci Technol,* 29(5) (2013) 626.

23 Hongguang Liu, Fuyong Cao, Guang-Ling Songa, Dajiang Zheng, Zhiming Shi, Mathew S Dargusch, & Andrej Atrens, J *Mater Sci Technol,* 35(9) (2019) 2003.

24 Liu R L, Scully J R, Williams G, Birbilis N, & Williams Geraint, *Electrochim Acta,* 260 (2018) 184.

25 Merson, Dmitry, Linderov Mikhail, Vasilev Evgenii, Markushev Mikhail, & Vinogradov Alexei, *Mater Lett,* 7(4) (2017) 421.

26 Mostaed Ehsan, Vedani Maurizio, Hashempour Mazdak, & Bestetti Massimiliano, *Biomatter,* 4(1) (2014) e28283.

27 Niinomi Mitsuo, Narushima Takayuki, & Masaaki Nakai, Advances in metallic biomaterials tissues, materials and biological reactions."*Heidelberg, DE: Springer* (2015).

28 Oungoulian Sevan R, Durney Krista M, Jones Brian K, Ahmad Christopher S, Hung Clark T, & Ateshian Gerard A, *J Biomech,* 48(10) (2015) 1957.

29 Pei Yanbo, Gui Yunwei, Huang Tao, Chen Fuxiao, Zhong Shiyu, & Song Zhuo, *Mater Res Express,* 7(6) (2020) 066525.

30 PeronMirco, Skaret Pal Christian, Fabrizi Alberto, Varone Alessandra, Montanari Roberto, Roven Hans Jørgen, Ferro Paolo, Berto Filippo, & Torgersen Jan, *J MechBehav Biomed Mater,* 101 (2020) 103429.

31 Prasad Soni, Ehrensberger Mark, Prasad Gibson Monica, Kim Hyeongil, & Monaco Jr Edward A, *J Oral Biosci,* 57(4) (2015) 192.

32 Rajendran Radha, & Sreekanth D, *J Magnes Alloy,* 5(3) (2017) 286.

33 Rahim Muhammad Imran, UllahSami, & Mueller Peter P, *Metals,* 8(7) (2018) 532.

34 Rahmatabadi Davood, TayyebiMoslem, HashemiRamin, & FarajiGhader, *Int J Miner Metall Mater,* 25(5) (2018) 564.

35 Saini, Monika, Singh Yashpal, Arora Pooja, Arora Vipin, & Jain Krati, *World J Clin Cases,* 3(1) (2015) 52.

36 Schwarz F, Eilers C, & Krüger L, *Mater Charact,* 105 (2015) 144.

37 Schwarz, Friederike, et al. "Microstructural and mechanical characterization of ARB AZ31." *Materials Science Forum*, Vol. 765. Trans Tech Publications Ltd, 2013.

38 Segal Vladimir, *Materials,* 11(7) (2018) 1175.

39 Song Guangling, Andrej Atrens, &David St John, *Essential readings in magnesium technology*, Springer, Cham, (2016) 565-572.

40 Su Lihong, Lu Cheng, Tieu AnhKiet, Deng Guanyu, & Sun Xudong, *Mater SciEng: A,* 559 (2013) 345.

41 Tong Xian, Zhang Dechuang, Zhang Xiaotuan, Su Yingchao, Shi Zimu, Wang Kun, Lin Jianguo, Li Yuncang, Lin Jixing, & Wen Cuie, *Acta Biomater,* 82 (2018) 197.

42 Toroghinejad, Mohammad Reza, Fakhreddin Ashrafizadeh, & Roohollah Jamaati, *Mater Sci Eng: A,* 561 (2013) 145.

43 Toth Laszlo S, & Chengfan Gu, *Mater Charact,* 92 (2014) 1.

44 Vinogradov Alexei, & Yuri Estrin, *Prog Mater Sci,* 95 (2018) 172.

45 Wan Peng, Lili Tan, & Ke Yang, *J Mater Sci Technol,* 32(9) (2016) 827.

46 Wu Huanchun, Li Chengtao, Fang Kewei, Zhang Wenqian, Xue Fei, Zhang Guodong, & Wang Xuelin, *Corros Mater,* 69(11) (2018) 1572.

47 Xu Wanqiang, Birbilis Nick, Sha Gang, Wang Yu, Daniels John E, Xiao Yang, & Ferry Michael, *Nat Mater,* 14(12) (2015) 1229.